



Nature and origin of an argillic horizon in a soil of the Boulder Batholith, Montana
by Paul Anderson McDaniel

A thesis submitted in partial fulfillment of the requirements for the degree of Master of Science in Soils
Montana State University

© Copyright by Paul Anderson McDaniel (1983)

Abstract:

Some forested soils of the granitic Boulder batholith in Montana have clay-rich horizons and are poorly drained. The purpose of this project was to study a representative soil of the area and determine the processes responsible for genesis of a clay-rich argillic horizon in coarse-grained granitic parent material. X-ray diffraction, thin section, and scanning electron microscopy techniques were used to do this.

Clay fractions from the B horizons of this soil differed markedly from surface horizons in both type and amount of clay minerals present. Smectite dominated the clay fraction and accounted for up to one-fourth of the fine-earth. Soil fabric analyses indicated pedogenic processes were not responsible for the high smectite content of the B horizon. The smectite is an in situ weathering product occurring in zones of weathering similar to those characteristic of hydrothermal alteration.

Hydrothermal alteration of quartz monzonite, a geological process, is apparently responsible for most of the chemical, physical, and mineralogical properties of the B horizon. Although effects of pedogenic processes of clay formation and clay movement (lessivage) can be seen, their influence on soil properties is minimal in these soils.

NATURE AND ORIGIN OF AN ARGILLIC HORIZON IN A SOIL
OF THE BOULDER BATHOLITH, MONTANA

by

Paul Anderson McDaniel

A thesis submitted in partial fulfillment
of the requirements for the degree

of

Master of Science

in

Soils

MONTANA STATE UNIVERSITY
Bozeman, Montana

March 1983

MAIN LIB.
N378
M141
cop. 2

APPROVAL

of a thesis submitted by

Paul Anderson McDaniel

This thesis has been read by each member of the thesis committee and has been found to be satisfactory regarding content, English usage, format, citations, bibliographic style, and consistency, and is ready for submission to the College of Graduate Studies.

3/4/83
Date

Gerald A. Nielsen
Chairperson, Graduate Committee

Approved for the Major Department

3/4/83
Date

Dwane L Miller
Head, Major Department

Approved for the College of Graduate Studies

3-7-83
Date

Michael Malone
Graduate Dean

STATEMENT OF PERMISSION TO USE

In presenting this thesis in partial fulfillment of the requirements for a master's degree at Montana State University, I agree that the Library shall make it available to borrowers under rules of the Library. Brief quotations from this thesis are allowable without special permission, provided that accurate acknowledgment of source is made.

Permission for extensive quotation from or reproduction of this thesis may be granted by my major professor, or in his/her absence, by the Director of Libraries when, in the opinion of either, the proposed use of the material is for scholarly purposes. Any copying or use of the material in this thesis for financial gain shall not be allowed without my written permission.

Signature

Paul McDaniel

Date

March 4, 1983

ACKNOWLEDGEMENTS

I would like to express my sincere appreciation to the following persons:

Dr. Gerald Nielsen, Dr. Larry Munn, Dr. Murray Klages, and Dr. Cliff Montagne for their support, encouragement, suggestions, and friendship while serving on my graduate committee.

Clint Mogen for his ideas and assistance with field sampling.

The U.S. Forest Service for their financial support of field work and Dave Ruppert, soil scientist for the Deerlodge National Forest, for his assistance.

Merrie Mendenhall for her help with the photographic aspects of this study.

Finally, the many people who have provided ideas, encouragement, and friendship during the course of this project.

TABLE OF CONTENTS

	Page
LIST OF TABLES	vii
LIST OF FIGURES.	viii
ABSTRACT	ix
INTRODUCTION	1
LITERATURE REVIEW.	2
Geology of the Boulder Batholith.	2
Argillic Horizon Formation on Granitic Parent Materials	3
Clay Movement	5
Hydrothermal Alteration of Granitic Parent Materials.	6
Smectite and Slope Failures	9
METHODS AND MATERIALS.	11
The Study Area.	11
Field Sampling and Characterization	11
Chemical Analyses	13
Physical Analyses	13
Clay Mineralogy.	14
Thin Section and Scanning Electron Microscopy	14
RESULTS.	16
Field Description and Characterization.	16
Physical Analyses	19
Chemical Analyses	21
Thin Section Analysis	22
Clay Mineralogy	27
Scanning Electron Microscopy.	32
DISCUSSION	35
Mineralogy and Soil Properties.	35
Mineralogy and Weathering	36
Evidence of Pedogenic Weathering.	37
Evidence of Clay Illuviation.	39
Evidence of Hydrothermal Alteration	39

TABLE OF CONTENTS--Continued

	Page
Soil Genesis	42
Hydrothermal Alteration and the Landscape	44
Conclusions	45
LITERATURE CITED	46
APPENDICES	51
APPENDIX	
I SOIL PROFILE AND SITE DESCRIPTION.	52
II PHYSICAL LABORATORY DATA	55
III CHEMICAL LABORATORY DATA	57
IV X-RAY DIFFRACTION PATTERNS FOR MG-SATURATED, ETHYLENE GLYCOL-SOLVATED CLAY FRACTIONS.	59
V ESTIMATED CLAY MINERAL PERCENTAGES	63

LIST OF TABLES

Table		Page
1	Average mineral composition of the Butte quartz monzonite	3
2	Estimated percentages of clay minerals from the A21, B22t, and C horizons	30
3	Estimated percentages of clay minerals from the B22t horizon, B22t matrix, and argillans from the B22t horizon.	32

LIST OF FIGURES

Figure	Page
1 Zones of hydrothermal alteration in quartz monzonite.	7
2 Maps showing location of the Boulder batholith and the study area.	12
3 Photograph of exposed soil profile used in this study	17
4 Diagrammatic representation of soil profile showing horizon designations and boundaries	17
5 Particle size distribution of A21, B22t, and C horizons.	20
6 Thin section from the C horizon.	23
7 Thin section from the A21 horizon	24
8 Thin section from the B22t horizon.	25
9 Thin section from the B22t horizon showing oriented clay.	26
10 Thin section of ghost rock inclusion showing plagioclase relict.	27
11 X-ray diffraction patterns of the clay fractions of the A21, B22t, and C horizons	29
12 X-ray diffraction patterns of the clay fractions of the B22t horizon, B22t matrix, and argillans from the B22t horizon	31
13 Scanning electron micrograph of dissolution pits on a feldspar grain taken from the B22t horizon.	34
14 Landscape following removal of overlying altered zones.	42
15 Soil horizon development following deposition, establishment of vegetation, and pedogenesis	43

ABSTRACT

Some forested soils of the granitic Boulder batholith in Montana have clay-rich horizons and are poorly drained. The purpose of this project was to study a representative soil of the area and determine the processes responsible for genesis of a clay-rich argillic horizon in coarse-grained granitic parent material. X-ray diffraction, thin section, and scanning electron microscopy techniques were used to do this.

Clay fractions from the B horizons of this soil differed markedly from surface horizons in both type and amount of clay minerals present. Smectite dominated the clay fraction and accounted for up to one-fourth of the fine-earth. Soil fabric analyses indicated pedogenic processes were not responsible for the high smectite content of the B horizon. The smectite is an in situ weathering product occurring in zones of weathering similar to those characteristic of hydrothermal alteration.

Hydrothermal alteration of quartz monzonite, a geological process, is apparently responsible for most of the chemical, physical, and mineralogical properties of the B horizon. Although effects of pedogenic processes of clay formation and clay movement (lessivage) can be seen, their influence on soil properties is minimal in these soils.

INTRODUCTION

This study originated, in part, as a result of field work conducted for the U.S. Forest Service. This field work involved examination and description of soils in an area of the Boulder batholith which was of particular interest to the Forest Service because of problems experienced with drainage and road bed stability.

Soils were examined in an attempt to relate their properties to unusual geomorphic features associated with poor drainage. Field work indicated zones of high clay contents in subsurface horizons of many soils in the study area. These clay zones were apparently responsible for impeded drainage in areas of the landscape.

The objective of this study was to characterize a representative soil of the area and determine the process or processes responsible for the clay-rich argillic horizon. To do this, x-ray diffraction, thin section, and scanning electron microscopy techniques were used to assess the effects of various pedogenic and geologic processes on the genesis of this soil.

LITERATURE REVIEW

Geology of the Boulder Batholith

The Boulder batholith is a large mass of igneous rock which was intruded under the earth's surface during the late Cretaceous and early Tertiary Periods, or approximately 68 to 78 million years ago (Tilling et al., 1968; Veseth and Montagne, 1980). Subsequent removal of up to 1.6 km of overlying sediments has exposed approximately 3900 square km (1500 square miles) of the batholith in southwestern Montana (Perry, 1962; Pinckney, 1965).

The predominant mineralogy of the Boulder batholith is quartz monzonite, a rock similar to granite but containing more plagioclase feldspar. The Butte quartz monzonite makes up approximately two-thirds of the exposed rock and is predominantly quartz monzonite with some granodiorite (Becraft et al., 1963; Tilling et al., 1968). In general, mineralogical and chemical compositions of different varieties of the Butte quartz monzonite are similar and differences are mainly seen in grain size, color, and fabric (Pinckney, 1965); Table 1 gives an average chemical composition for the Butte quartz monzonite based on findings of several researchers.

Table 1. Average mineral composition of the Butte quartz monzonite.

Quartz	25 %
Orthoclase	25 %
Plagioclase	35 %
Biotite	10 %
Hornblende	5 %
and other minerals	

(After Hood, 1963; Smedes, 1966; Becraft et al., 1963; Kaczmarek, 1974).

The quartz monzonite tends to be rather coarse-grained with individual mineral grains typically averaging 1 to 3 mm in diameter (Ruppel, 1963; Becraft et al., 1963). Phenocrysts of potassium feldspar with diameters up to 2.5 cm are common (Veseth and Montagne, 1980).

Argillic Horizon Formation on Granitic Parent Materials

An argillic horizon is defined by Soil Taxonomy (Soil Survey Staff, 1975) as "an illuvial horizon in which layer-lattice silicate clays have accumulated by illuviation to a significant extent". Since igneous crystalline rocks such as those found on the Boulder batholith generally have little or no clay-size material, some clay formation must precede or occur with argillic horizon formation. Clay formation occurs as primary minerals are altered by chemical and physical weathering processes.

Soil development on granitic parent materials is often preceded by formation of grus, a process known as grussification. The term grus refers to small, angular fragments of weathered rock which are larger than 2 mm. Chemical and physical alteration of biotite and

perhaps feldspar minerals appears to be the primary mechanism by which grussification of coarse-grained igneous rock occurs.

Several researchers have demonstrated the presence of partially altered biotite in grus. Apparently, alteration of biotite to secondary illite and vermiculite and the accompanying increase in volume are responsible for fracturing the parent material (Warhaftig, 1965; Nettleton et al., 1968; Isherwood and Street, 1976; Clayton et al., 1979).

Freeze-thaw cycles are probably an especially important physical weathering process in formation of grus in cold and dry climates. Increases in volume of 9% which accompany freezing of water can provide sufficient pressures to fracture most rocks (Birkeland, 1974).

The most important process of chemical weathering of common silicate and aluminosilicate minerals is hydrolysis (Birkeland, 1974). However, in cold, dry mountainous regions, the role of hydrolysis in clay formation is minimal (Millot, 1979). Jenny (1935) reported a linear relationship between clay formation and moisture and an exponential relationship between clay formation and temperature. In view of this, little clay formation would be expected in soils of the Boulder batholith under present climatic conditions.

Time is an important factor in argillic horizon formation, since both clay formation and translocation will increase with time. Ruppel (1962) studied Pleistocene ice movement in the northern part of the Boulder batholith and concluded that glacial deposits in the area ranged in age from early-Wisconsin to late-Wisconsin. This would put an approximate age on the landscape of anywhere from 100,000 to 10,000

years. Birkeland (1974) estimated the time required for minimal expression of a textural B horizon to be on the order of 1,000 years and 500,000 years for maximal expression. He has also reported a general lack of B horizons in soils formed in late-Wisconsin tills.

Clayton et al. (1979) reported that sediment yield studies indicated erosion losses averaging 1 cm per 1,000 years under present climatic conditions on the Idaho batholith. They felt that with this rate of erosion on slopes, there had not been enough time for modal development of argillic B horizons. Soil profile descriptions from their study area seem to support this hypothesis--argillic horizons are weakly expressed and restricted to soils formed on alluvium or colluvium with slope gradients less than 10% (Clayton, 1974).

Clay Movement

Evidence for translocation of clay minerals includes the presence of clay films or argillans on surfaces of peds and individual mineral grains. Argillans can be seen in some cases with the unaided eye or by use of a hand lens as well as by thin section analysis. Argillans observed in thin section exhibit a finer, more homogenous texture and differ in their birefringence and extinction patterns compared to the soil matrix when viewed under cross-polarized light (McKeague and St. Arnaud, 1969).

However, oriented clay particles along voids and ped surfaces can be caused by stress or pressure and not illuviation of clay (Birkeland, 1974). Clay films may also be destroyed and incorporated

into the soil matrix by shrinking and swelling action of 2:1 expansible clay minerals (Nettleton et al., 1969) and possibly by mixing of soil by roots and fauna.

Numerous researchers have observed clay films in portions of B horizons of soils on granitic parent materials in mountainous regions of the western United States, including the Boulder batholith. However, these argillans are generally poorly expressed, indicating the lack of development in most of these soils, (Hood, 1963; Marchand, 1974; Clayton et al., 1979; Veseth, 1981).

In general, soils of the Boulder batholith show little development. The coarse texture and mineralogical composition of the parent material tends to yield soils that are coarse-textured and low in clay content. Clay-sized mica (illite and sericite) and kaolinite mineral assemblages are dominant in the clay fraction of batholith soils (Hood, 1963; Veseth, 1981).

Hydrothermal Alteration of Granitic Parent Materials

Hydrothermal alteration of granitic parent material can have a significant effect on subsequent pedogenic processes. Hydrothermal activity can greatly accelerate chemical weathering processes and alter normal weathering products. This activity has been reported over extensive areas of the Boulder and Idaho batholiths.

Sales and Meyer (1948) were among the first researchers to study hydrothermally altered granite in detail on the southern part of the Boulder batholith near Butte, Montana. They described distinct mineralogical zones or reaction rims representing zones of diminishing

hydrothermal activity extending outward from joints and fractures. These distinct mineralogical zones were probably caused by changes in the composition of hydrothermal solutions as reactions occurred in host rocks (Grim, 1968). Alteration most likely occurred as the batholith cooled, creating a network of fractures and cracks through which hydrothermal fluids circulated (Pinckney, 1965). Becraft et al. (1963) and Pinckney (1965) also observed similar alteration zones in central and northern portions of the Boulder batholith.

Figure 1 shows a simplified diagram of hydrothermal alteration zones in quartz monzonite. Zones shown in Figure 1 can occur over distances ranging from only a few centimeters to several kilometers and represent a horizontal extension of a larger alteration zone with vertical orientation.

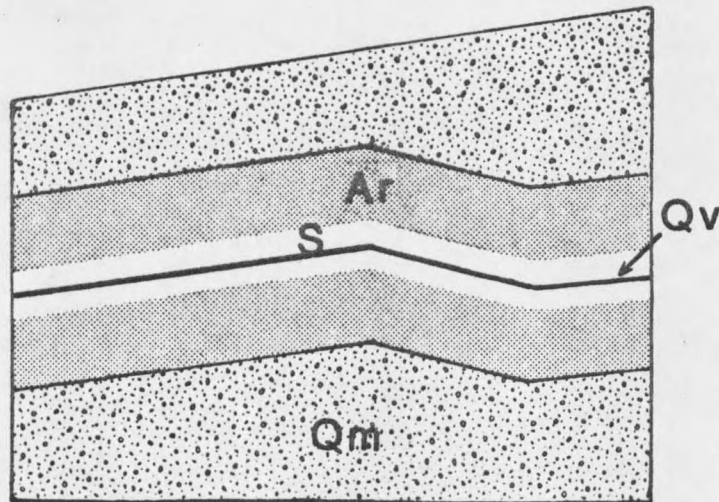


Figure 1. Zones of hydrothermal alteration in quartz monzonite. Qv = quartz or chalcedony vein; S = sericitized zone; Ar = argillized zone; Qm = unaltered quartz monzonite.

The quartz or chalcedony vein represents the zone of most intense alteration and reflects the original structure of the cracks or joints. Extending outward from the vein is a less-altered sericitized zone which contains moderately altered quartz grains, extensively altered potassium feldspars, and completely altered plagioclase, biotite, and hornblende grains. Iron pyrite, quartz, and sericite are the dominant alteration products (Sales and Meyer, 1948; Becraft et al., 1963).

An argillized zone envelopes the sericitized zone and is characterized by less intense alteration. The argillized zone is composed of a kaolinitic subzone and a less-altered montmorillonite (smectite) subzone. Quartz and potassium feldspars show little or no alteration, but plagioclases, biotite, and hornblende are extensively to completely altered to a variety of products (Guilbert and Sloane, 1968).

Montmorillonite is the dominant weathering product in the montmorillonitic subzone, occurring primarily as an alteration product of plagioclase, biotite, and hornblende (Becraft et al., 1963; Pinckney, 1965; Sales and Meyer, 1948). Illite and kaolinite also occur in this subzone in lesser amounts. The intensity of alteration in the montmorillonitic subzone is usually gradational over a distance of a few meters and is usually the widest of all alteration bands (Pinckney, 1965).

Only slight alteration is seen in quartz monzonite beyond the montmorillonite subzone. Plagioclase, biotite, and hornblende can be partially altered, with chlorite being the dominant alteration product

along with minor amounts of montmorillonite (Becraft et al., 1963; Guilbert and Sloane, 1968).

Hood (1963) and Clayton et al. (1979) have described mineralogical properties of soils formed in areas of hydrothermal alteration on the Boulder and Idaho batholiths. Hood described yellow clay zones in association with areas of hydrothermal alteration. He identified this yellow clay as smectite by x-ray diffraction techniques.

Clayton et al. (1979) also found montmorillonite in the clay fraction of soils from areas of hydrothermal alteration. Kaolinite and illite dominated the clay-size fraction of soils from other areas of more intense hydrothermal alteration. Examination of soil thin sections revealed that plagioclase feldspars had undergone extensive internal alteration to sericite (kaolinite, illite, and montmorillonite) and orthoclase minerals were clouded and sericitized along fractures. This alteration of feldspar was more pronounced than that seen in soils from areas of the batholith unaffected by hydrothermal alteration.

Smectite and Slope Failures

Because of a relatively low layer charge, smectites can expand and adsorb several times their weight in water (Borchardt, 1979). This along with their adhesive and cohesive properties causes smectite to frequently be associated with landslides, soil creep, and poor drainage.

Hydrothermally altered bedrock has been implicated in slope failures on the Idaho batholith (Clayton et al., 1979). Soil movement

appears to be related to poor drainage associated with argillized zones and frequently occurs during spring snowmelt. Orientation of clay seams with the slope is probably important in determining the extent and type of mass movement.

METHODS AND MATERIALS

The Study Area

During the summer of 1980, 35 pedons were examined and characterized in a 10 square km area of the Deerlodge National Forest approximately 8 km southwest of Boulder, Montana. Figure 2 shows the location of the study area.

One pedon from the area was selected for this study on the basis of field characterization. This pedon contained an argillic horizon which exhibited properties representative of those of other soils occurring within the study area. These included B horizons with irregular and broken boundaries, strong chromas, the presence of "ghost rocks", and a sizeable increase in the amount of clay-size material when compared to the overlying and underlying horizons.

Field Sampling and Characteristics

A pit was dug to expose a soil profile 1.5 m across and 2 m deep. Field characterization and sampling were done using guidelines established in Soil Taxonomy (Soil Survey Staff, 1975) and Soil Survey Manual (Soil Survey Staff, 1951) with the assistance of Clint Mogen, retired USDA-SCS state soils correlator for Montana. Samples were collected from all soil horizons as well as from "ghost rock" inclusions found within the soil profile. Soil samples were air-dried, ground in a flail-type grinder, sieved to remove the greater than 2 mm

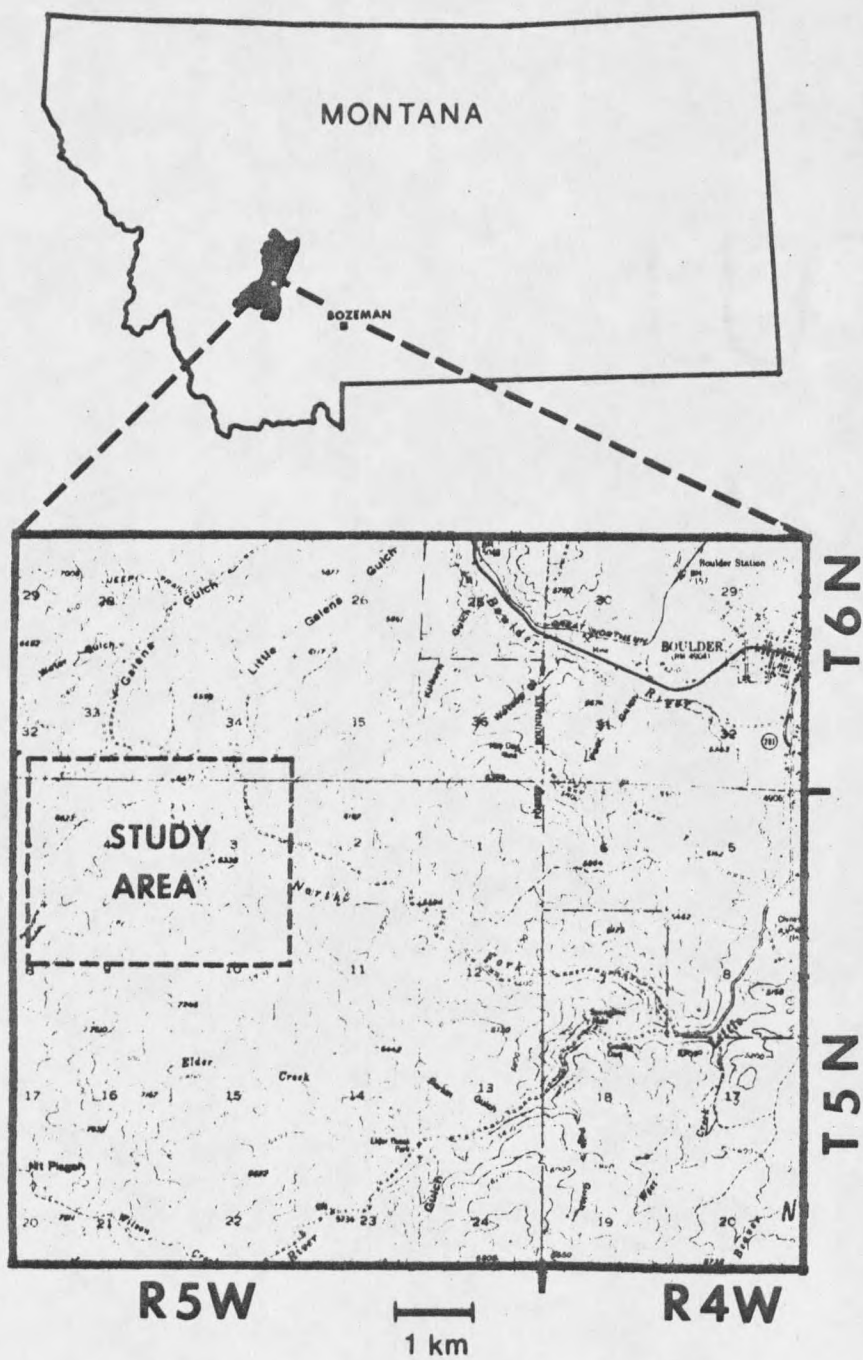


Figure 2. Maps showing location of the Boulder batholith and the study area.

fraction, and subsampled for laboratory analyses. Undisturbed samples from each horizon were used for soil fabric analysis.

Chemical Analyses

Soluble cation content, sodium adsorption ratio (SAR), electrical conductivity, pH of saturated paste, and water content at saturation were measured according to methods in Agriculture Handbook 60 (U.S. Salinity Laboratory Staff, 1969). Soil organic matter content was determined colorimetrically (Sims and Haby, 1971). A Perkin-Elmer model 303 atomic absorption spectrophotometer was used to measure soluble base cations (Ca, Mg, Na, K), extractable base cations (Chapman, 1965a), and cation exchange capacity (Chapman, 1965b). Total nitrogen was determined using a semi-micro Kjeldahl method (Bremner, 1965).

Physical Analyses

Fine earth fractions of samples were dispersed with sodium hexametaphosphate (Day, 1965) using a Blackstone BP2B ultrasound apparatus. Particle size analysis and separations were done by pipette method using particle settling time nomographs from Jackson (1956). In addition, percentages of the various sand-size fractions and coarse fragment contents were determined gravimetrically using appropriate sieves. Water content of the fine-earth fraction at 1/3 and 15 bar tension was measured using a ceramic plate apparatus and a pressure membrane apparatus, respectively (U.S. Salinity Laboratory Staff, 1969).

Clay Mineralogy

Clay mineralogy of the clay-size fraction of all samples was determined by x-ray diffraction analysis. Slides were prepared using a paste method (Thiesen and Harward, 1962), analyzed on a General Electric XRD-5 x-ray diffraction machine, and interpreted using techniques described by Whittig (1965). Semi-quantitative analysis of x-ray diffraction data was used to estimate relative amounts of various clay minerals present in each sample (Klages and Hopper, 1982).

In addition, clay mineralogy of argillans and clay-size matrix taken from the argillic horizon was determined. Clay films viewed under a binocular microscope were scraped from ped surfaces with a razor blade. Interiors of peds were sampled to obtain matrix material. Clay mineralogy of these samples was determined using x-ray diffraction techniques previously described.

Thin Section and Scanning Electron Microscopy

Thin sections of selected soil horizons were prepared by Cal-Brea Geological Services in Anaheim, California. Thin sections were examined and described under a petrographic microscope using techniques described by Moorhouse (1959) and FitzPatrick (1980).

Selected samples were examined using scanning electron microscopy (SEM). Samples of undisturbed and untreated soil material were used. Samples were prepared by Mr. Andy Blixt and examined at the Montana

Agricultural Experiment Station SEM laboratory at Montana State University in Bozeman.

RESULTS

Field Description and Characterization

The soil profile selected for this study is shown in Figures 3 and 4. Many of the features characteristic of soils in the study area are present in this profile and will be discussed in detail. A complete profile description is in Appendix I.

Based on field characterization this soil was classified as a fine-loamy over sandy, mixed Mollic Cryoboralf. Mean annual and mean summer soil temperatures were estimated using predictions of Munn and Nielsen (1979). Mollic subgroup classification was based on moist color values of 3 in the surface eluvial horizons (Soil Survey Staff, 1975).

The argillic horizon present in this soil exhibited some rather striking features. A sizeable increase in clay-sized material was observed in the argillic horizon compared with the surface eluvial horizons. The eluvial horizons were sandy loams whereas the argillic horizon was a sandy clay loam. Prismatic structure could be seen in the B22t and B23t horizons and clay films were visible on many ped faces. Boundaries of the Bt horizons and the B3 horizon were broken and discontinuous across the face of the exposed profile. The unusual diagonal orientation of the B3 boundary can be seen in Figures 3 and 4.



Figure 3. Photograph of exposed soil profile sampled in this study.

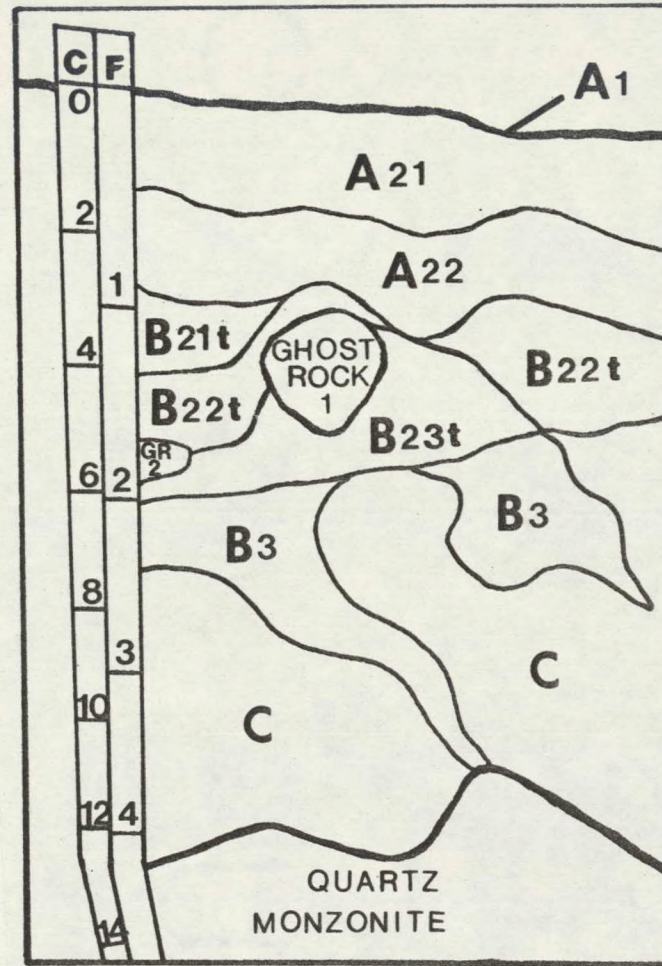


Figure 4. Diagrammatic representation of soil profile showing horizon designations and boundaries. GR 2 = Ghost Rock 2.

Munsell color determinations were somewhat difficult because of the "salt and pepper" appearance of coarse-grained granitic parent material. However, strong chromas were characteristic of the B horizons, particularly the B3.

Wet and dry consistence of the B horizons differed markedly from that of the eluvial and C horizons. Peds from the argillic horizon were hard or very hard when dry and sticky and plastic when wet. These properties were not seen in the A or C horizons. The B3 horizon was also noticeably more sticky and plastic than the A horizons, while having a very similar texture.

One of the more unusual characteristics of the argillic horizon was the presence of inclusions of coarser-textured, plastic material. One of these inclusions or "ghost rocks" can be seen in Figure 3 as the grayish material in the center of the profile at a depth of about 45 cm. This ghost rock had a diameter of 15 cm. Another ghost rock was also present in the lower portion of the B23t horizon. Both of these inclusions were carefully sampled for physical, chemical, and mineralogical analyses.

The study site was located at an elevation of 1950 m (6400 ft) on a south-facing ridge slope of 18%. Vegetation was characterized as being of the Pseudotsuga menziesii (Douglas fir)/ Calamagrostis rubescens (pinegrass) habitat type, Arctostaphylos uva-ursi (kinnickinnick) phase (after Pfister et al., 1977).

Complete results of chemical and physical analyses are summarized in Appendices II and III. Results of some of these analyses are presented in the following sections.

Physical Analyses

Particle size analysis of fine-earth fractions of soil horizons confirmed field textures and the presence of clay-enriched illuvial horizons. Figure 5 shows particle size distribution curves for the A21, B22t, and C horizons. Increasing particle diameter is plotted on a logarithmic scale as a summation percentage. Each point on the curve gives the percent of the fine earth fraction for that horizon which has a particle diameter equal to or smaller than that given on the X axis. The steeper slopes of particle size distribution curves for the A21 and C horizons are indicative of the coarser textures of these horizons.

The B21t, B22t, and B23t horizons contained 20, 28, and 16% clay-sized material, respectively, and had sandy loam and sandy clay loam textures. These illuvial horizons contained approximately 2 to 4 times as much clay as did the surface eluvial horizons.

The A21 and A22 horizons both had sandy loam textures and contained 6 and 8% clay, respectively. The C horizon had a sand texture with less than 2 percent clay. The difference in texture between the argillic and C horizons resulted in the fine-loamy over sandy textural family designation.

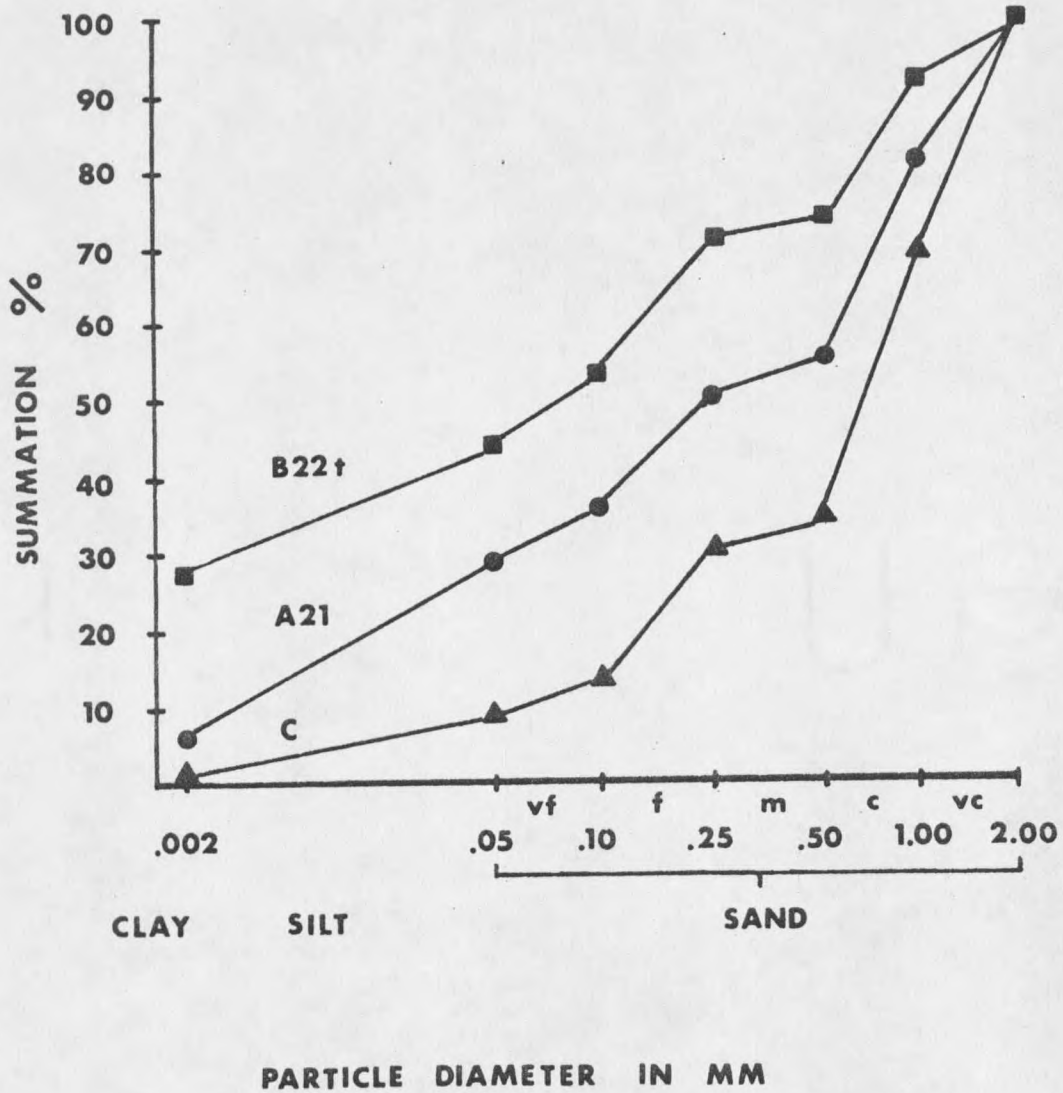


Figure 5. Particle size distribution of the A21, B22t, and C horizons.

Ghost rocks 1 and 2 contained 8 and 9% clay, respectively. These clay percentages are considerably less than those of the B22t or B23t horizons from which these inclusions were sampled.

Highest coarse fragment content was found in the C horizon. On a weight basis, almost 40% of this horizon was composed of grus material larger than 2 mm.

Soil moisture retention was highest in illuvial Bt horizons as would be expected on the basis of clay content. It is interesting to note that the B3 horizon retains more soil water but contains about the same amount of clay-sized material and less silt-sized material than the A21 and A22 horizons. This suggests different clay mineralogies in the eluvial and B3 horizons and that B horizon clays have greater water retention capabilities.

Chemical Analyses

As might be expected, pH values increased with depth in the soil profile. pH values ranged from 4.8 (very strongly acid) in the A21 horizon to 6.1 (slightly acid) in the C horizon. The pH of the argillic horizon ranged from 5.3 in the B21t to 5.7 in the B23t. pH values of 6.2 were obtained for both ghost rock samples taken from the argillic horizon. These pH's were more similar to that of the C horizon than to those of the B22t and B23t horizons in which these inclusions were found.

Cation exchange capacity (CEC) was highest in the argillic horizon. CEC's of 21.2, 31.9, and 24.5 me/100 g were measured for the

B21t, B22t, and B23t horizons, respectively. These CEC values reflect higher clay contents found in these horizons.

Organic matter content was less than 1% for all horizons except the thin surface A1, which contained 6.8% organic matter by weight. The B22t horizon contained the most organic matter (0.7%) of any of the subsurface horizons, perhaps due to illuviation. Organic staining was observed in argillans found on ped surfaces in this horizon.

Thin Section Analysis

Examination of thin sections indicated major differences in weathering between the argillic horizon and the eluvial and C horizons.

There was little visual evidence of weathering in the C horizon. Figure 6 shows large mineral grains in a closely packed arrangement similar to rock structure. Biotite and hornblende appeared relatively fresh except for slight alteration which could be seen on the edges of these mineral grains. Plagioclase, orthoclase, and quartz appeared mainly as subhedral crystals, and except for some fractures, showed little or no evidences of weathering.

Thin section examination of the eluvial horizons showed a general decrease in mineral grain size (Figure 7). Compared to mineral grains seen in the C horizon, biotite and hornblende exhibited evidences of more chemical weathering. This alteration was seen as a loss of pleochroism along the fringes of these mineral grains.

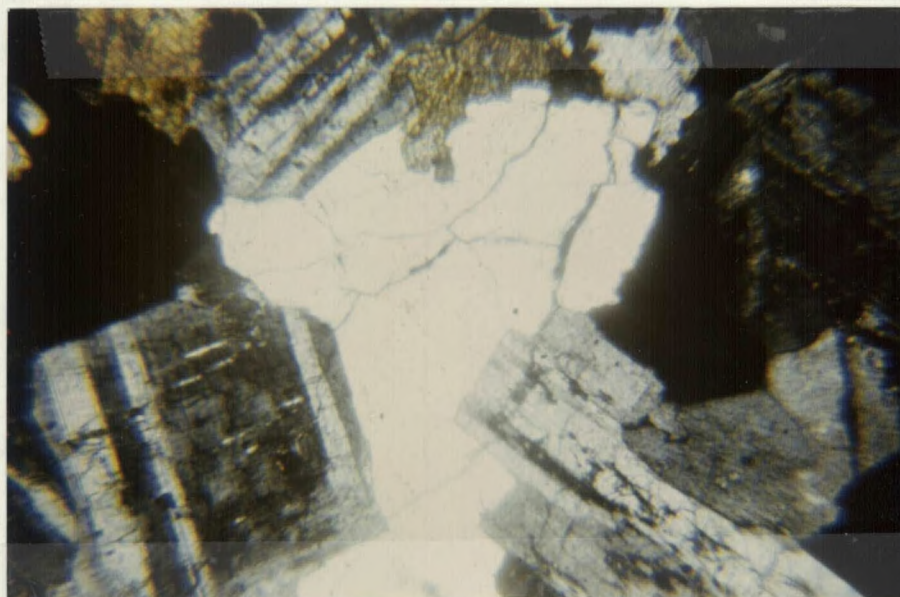


Figure 6. Thin section from the C horizon. Crossed polarizers, X 160. A large fractured quartz grain is located in the center. Plagioclase shows characteristic twinning, seen as alternating light and dark bands.

Plagioclase feldspars showed more fracturing and alteration to clay minerals. Illite and/or smectite could be seen along many of these fractures as well as on mineral grain edges. Orthoclase grains were smaller than in the C horizon but showed only slight evidence of chemical weathering. Quartz grains were fractured, but otherwise appeared unweathered.

Figure 8 shows a thin section view of the B22t horizon. A more advanced stage of weathering is indicated in this horizon by the lack of fresh biotite, hornblende, and plagioclase. These minerals have been altered, forming a yellow, clay-rich matrix which encloses large orthoclase and quartz grains. Almost no evidence remained of the original mineral arrangement as seen in the C horizon.

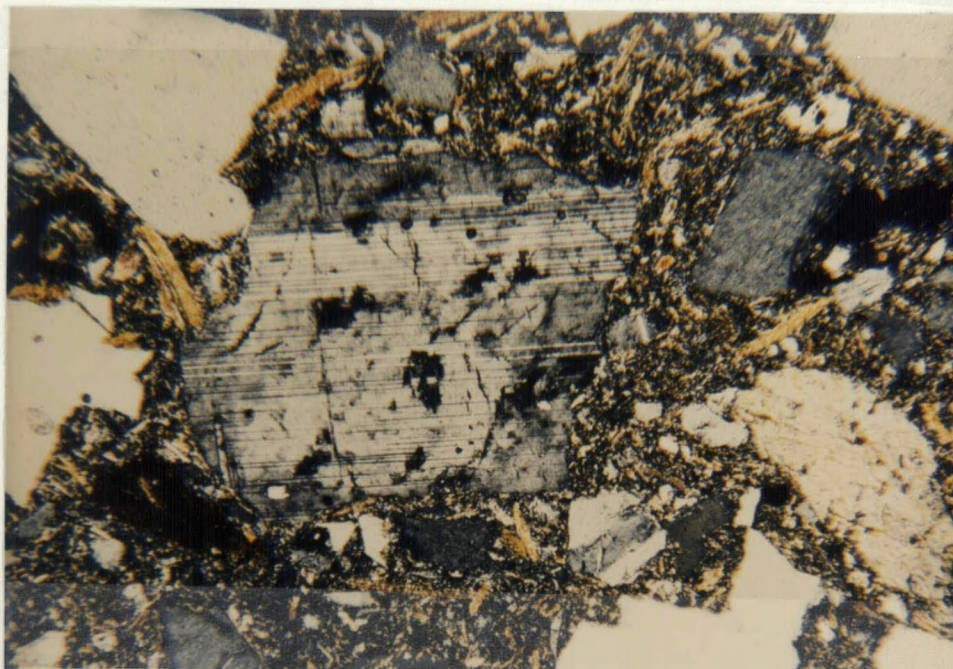


Figure 7. Thin section of A21 horizon. Crossed polarizers, X 160. Some clay is seen as fine-grained, yellowish material in the soil matrix.

Perhaps the most striking feature in examining thin sections of the B21t, B22t, and B23t was the general lack of identifiable plagioclase grains. This seemed to suggest more intense weathering had occurred in the argillic horizon than in the A2 or C horizons. The more intensely altered plagioclase was apparently responsible for the clay-rich matrix of the argillic horizon.

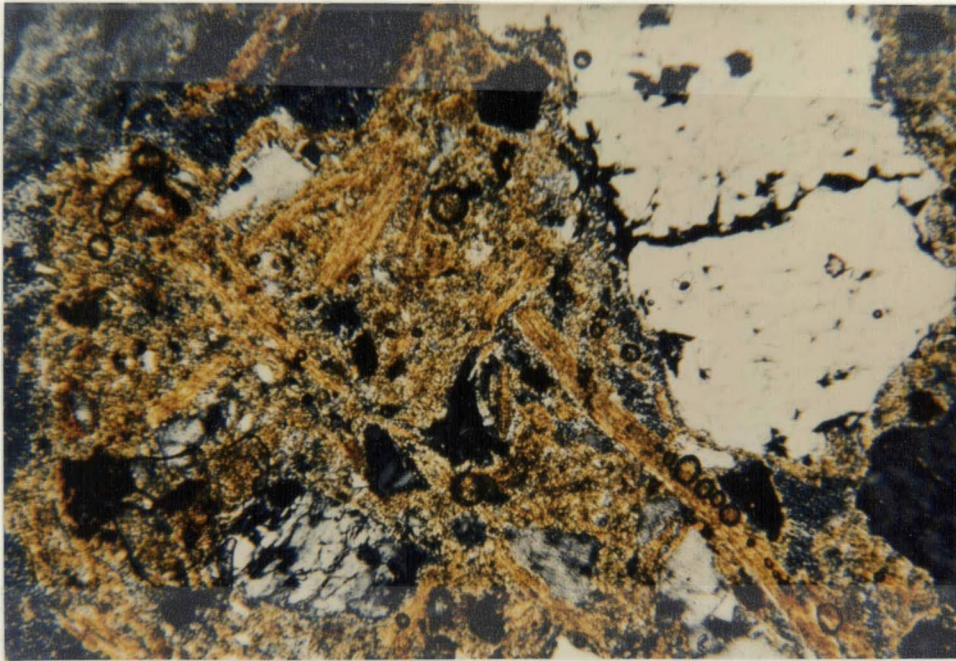


Figure 8. Thin section from the B22t horizon. Crossed polarizers, X 160. Yellowish, clay-rich matrix encloses larger quartz and orthoclase grains.

Evidences of translocated clay were also observed in thin sections of the B22t and B23t horizons. This clay was seen as yellowish, fine-grained, strongly birefringent laminations on quartz and feldspar grains (Figure 9). Oriented clay was found in the B22t and B23t horizons, but it appeared to represent only a small fraction of the total soil volume.

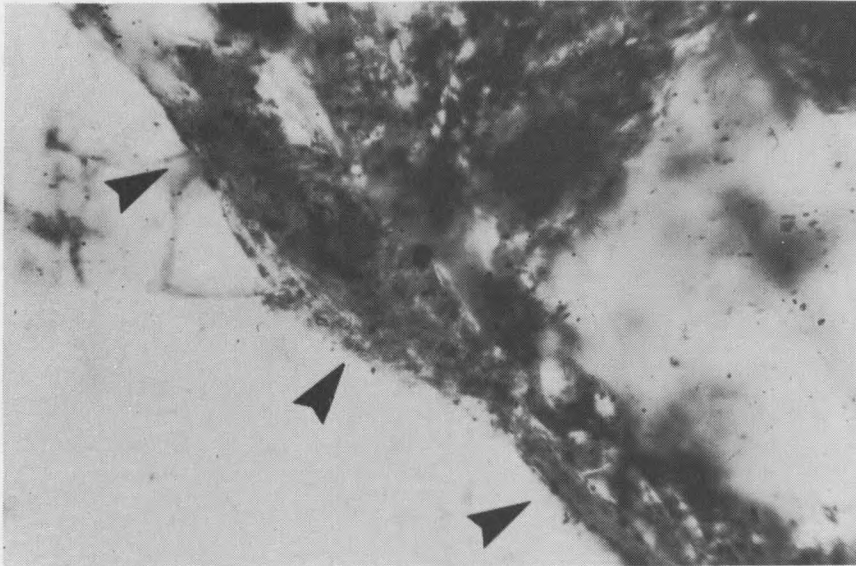


Figure 9. Thin section from the B22t horizon showing oriented clay. Crossed polarizers, X 1600. Arrows show laminations of oriented clay coating a quartz grain.

Thin section analysis of ghost rock material showed weathering characteristics similar to those observed in the argillic horizon, and also revealed the presence of plagioclase relicts (Figure 10). These plagioclase grains exhibited partial replacement by fine-grained, highly birefringent clays, but the original subhedral crystalline structure was still evident. In general, chemical weathering processes appeared to be less intense than those seen in the B22t horizon, but more intense than in the A or C horizons.



Figure 10. Thin section of ghost rock inclusion showing plagioclase relict. Crossed polarizers, X 200. Dashed white line shows original crystalline structure of plagioclase grain which is still evident despite intensive alteration to finer-grained material.

To summarize results of thin section analysis, weathering was more evident in B horizons than in A or C horizons. The B22t horizon exhibited the most intense alteration of plagioclase, biotite, and hornblende, resulting in a clay-rich matrix.

Clay Mineralogy

Mineralogy of the clay-size fraction was determined for all samples. X-ray diffraction results indicated that different clay mineral assemblages are found within the soil profile. Differences

between A and B horizons were particularly apparent and are discussed in some detail. X-ray diffraction patterns for all samples are in Appendix IV.

Figure 11 shows the x-ray diffraction patterns for the A21, B22t, and C horizons. Diffraction patterns are for Mg-saturated, ethylene glycol-solvated samples. The diffraction pattern for the clay fraction of the A21 horizon is dominated by a peak corresponding to a basal spacing of 10 A, characteristic of the illite minerals. By contrast, a very strong peak corresponding to a basal spacing of 17 A dominates the diffraction pattern of the B22t horizon. This peak is characteristic of the smectite minerals (Whittig, 1965).

Diffraction data for the C horizon indicates the presence of both smectite and illite clay minerals. The 14 A peak in the diffraction patterns of the A21 and C horizons collapsed to 10 A upon saturation of samples with K and heating to 500 degrees C for 2 hours. This indicated the presence of vermiculite. Vermiculite was not detected in any of the B horizons.

Semi-quantitative estimates of the various clay mineral percentages in each sample were made by calculating areas underneath diffraction peaks. Areas were adjusted using methods of Klages and Hopper (1982) to give estimated relative mineral percentages. Appendix V shows relative clay mineral percentages for all samples. Relative amounts of clay minerals found in the A21, B22t, and C horizons are given in Table 2.

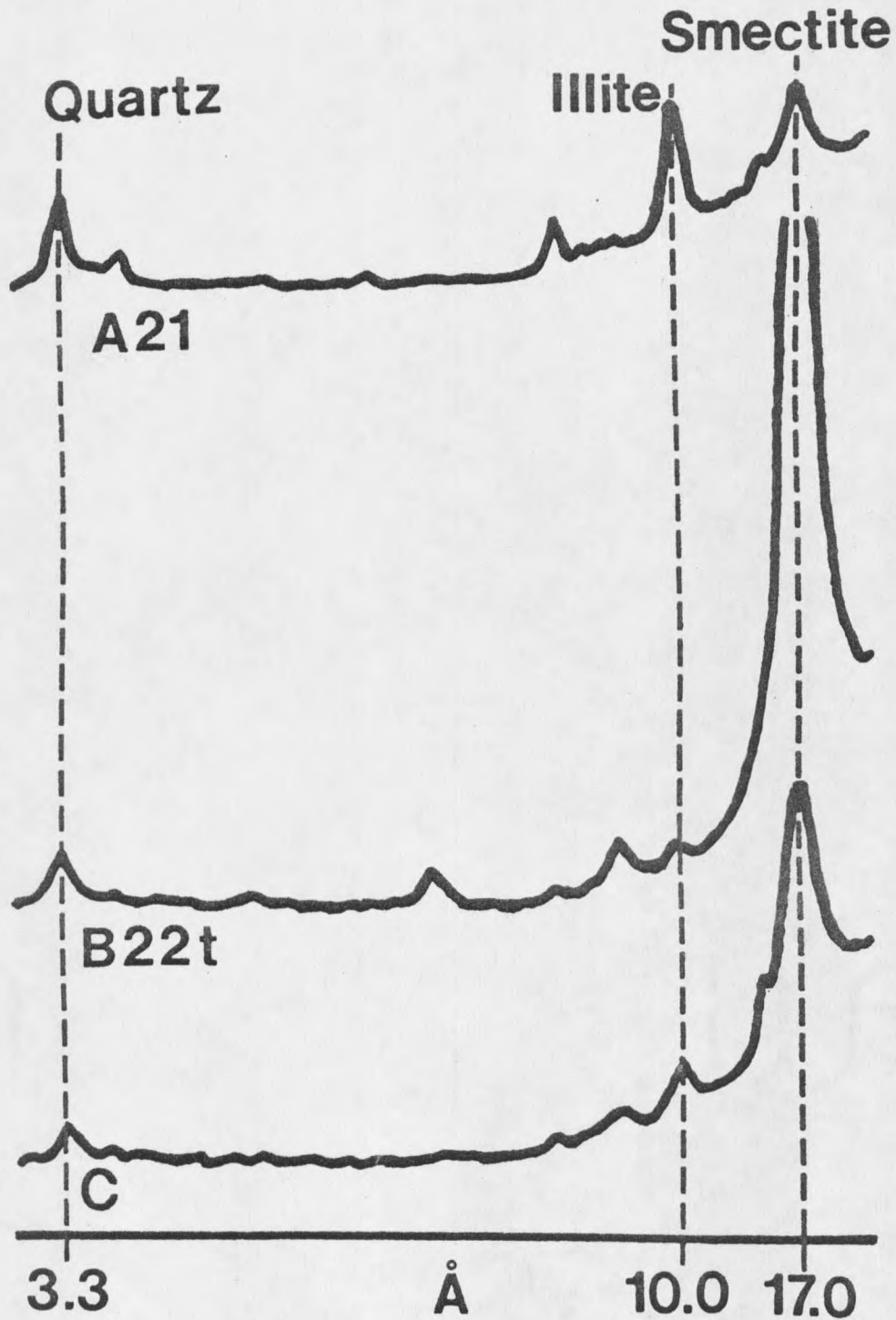


Figure 11. X-ray diffraction patterns of the clay fractions of the A21, B22t, and C horizons. Samples were Mg-saturated and solvated with ethylene glycol.

Table 2. Estimated percentages of clay minerals from the A21, B22t, and C horizons.

	<u>Smectite</u>	<u>Illite</u>	<u>Vermiculite</u>	<u>Kaolinite</u>	<u>Quartz</u>
A21	9	79	3	9	-
B22t	83	14	-	1	3
C	32	52	7	-	9

Results indicate that illite dominates the A21 horizon, accounting for approximately 79% of the clay fraction. In sharp contrast to this, smectite accounts for approximately 83% of the clay fraction of the B22t horizon. Illite dominates the C horizon, comprising over half of the clay fraction.

An attempt was made to determine to what extent the process of lessivage (clay eluviation and illuviation) had influenced the contrasting mineralogy and texture of the argillic horizon. Clay films were scraped from surfaces of peds taken from the B22t horizon and analyzed using x-ray diffraction techniques. X-ray analysis was also performed on the clay-size portion of the soil matrix, which was obtained from the interior of peds taken from the B22t horizon. Figure 12 shows x-ray diffraction patterns for these two components of the soil fabric. The diffraction pattern for the whole B22t horizon, in which these two components are combined, is also included. Semi-quantitative estimates of clay mineral percentages are given in Table 3.

These data show clay films to be primarily illite with smectite also being present in smaller amounts. Clay mineralogy of the matrix

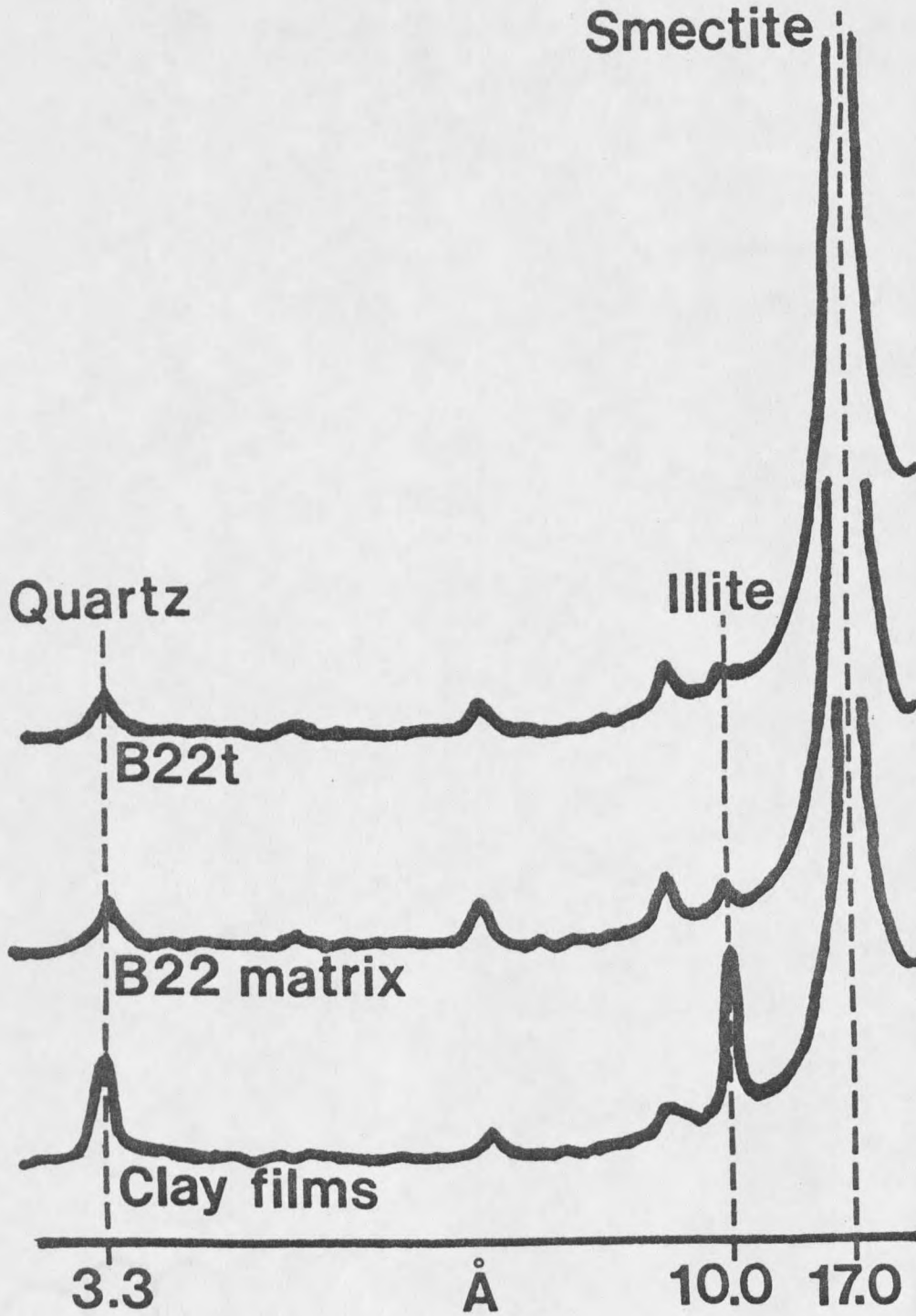


Figure 12. X-ray diffraction patterns of the clay fractions of the B22t horizon, B22t matrix, and argillans from the B22t horizon. Samples were Mg-saturated and solvated with ethylene glycol.

Table 3. Estimated percentages of clay minerals from the B22t horizon, B22t matrix, and argillans from the B22t horizon.

	<u>Smectite</u>	<u>Illite</u>	<u>Vermiculite</u>	<u>Kaolinite</u>	<u>Quartz</u>
B22t	83	14	-	1	3
B22t Matrix	87	7	-	-	6
Argillans	42	58	-	-	-

of the matrix of the B22t horizon is very similar to that of the horizon as a whole--smectite is dominant with small amounts of illite, kaolinite, and quartz present. Based on these data, illite appears to be the dominant clay mineral being transported within the soil profile.

Smectite was the dominant clay mineral in all B horizons as well as in the ghost rocks (Appendix V). Clay mineral assemblages for these horizons in order of decreasing amounts are smectite-illite-quartz-kaolinite. An illite-smectite-kaolinite-vermiculite clay mineral assemblage is present in both the A21 and A22 horizons. The C horizon contains an illite-smectite-quartz-vermiculite clay mineral suite.

Scanning Electron Microscopy

Scanning electron microscopy (SEM) imagery was somewhat difficult to interpret, but some recognizable features were observed. SEM imagery of C horizon material showed a general lack of pore space. Sharp, well-defined outlines of mineral grains were seen. Imagery from A horizons appeared similar although more pore space was evident.

By contrast, mineral edges appeared somewhat rounded and poorly defined in samples from the B22t horizon. The lack of striking features observed in this horizon is perhaps due to clay coatings on the mineral surfaces. Also, Borchardt (1979) reported that smectite is notoriously nonphotogenic and the B22t horizon is rich in this clay mineral.

Distinctive weathering features were observed on feldspar mineral grains. Figure 13 is an electron micrograph of the surface of an orthoclase grain taken from the B22t horizon showing the presence of small pits. These pits are seen as a honeycomb structure and are similar in appearance to those described by several researchers (Bisdom, 1980). These weathering or dissolution pits were found in samples from both the A22 and B22t horizons. However, the occurrence of these features was limited and they probably do not represent a very significant amount of the total soil volume.

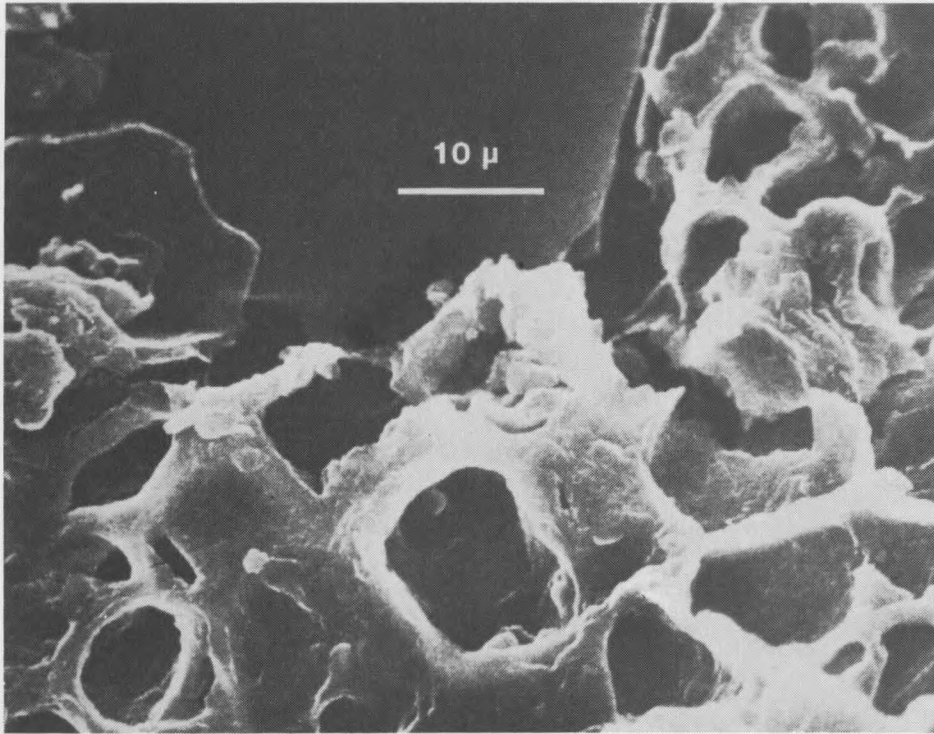


Figure 13. Scanning electron micrograph of dissolution pits on a feldspar grain taken from the B22t horizon. X 2000.

DISCUSSION

Results of this study reveal contrasting physical, chemical, morphological, and mineralogical characteristics among the horizons of this soil profile. This section will attempt to relate these characteristics to the genesis of this soil, and in particular, the argillic horizon.

Mineralogy and Soil Properties

Perhaps the single factor which most influences the properties of this soil is its mineralogy. Interpretation of x-ray diffraction data showed sharply contrasting clay mineralogy between the argillic horizon and eluvial and C horizons. Both the type and amount of clay minerals present in these horizons is different.

The differences in mineralogy influence morphological characteristics. Strong chroma, well-developed structure, and plastic consistency are field indicators of the mineralogy differences seen in the argillic horizon. Chemical and physical properties such as CEC, texture, and water-holding capacity also reflect differences in type and amount of clay minerals present.

Mineralogy and Weathering

The A21 and A22 horizons were similar in chemical, physical, morphological, and mineralogical properties and their genesis is presumably similar. The relatively low percentage of clay-size material in these horizons seems to indicate a rather early stage of weathering and soil development. The dominance of illite in the clay mineral fraction also supports this observation. Jackson (1959) reported that clay-size micas (illite) are generally more prevalent in clay fractions of less-weathered soils because they are largely inherited from parent material. The occurrence of illite with smectite, kaolinite, and vermiculite is consistent with clay mineral assemblages found by other researchers in soils from similar parent material formed under similar climatic conditions (Clayton, 1974; Marchand, 1974; Isherwood and Street, 1976; Veseth, 1981).

The presence of vermiculite is interesting in that it was not detected in the B horizons. It is generally accepted that vermiculite is formed almost exclusively by alteration of mica (Douglas, 1979). Therefore, its presence in the eluvial horizons (and C horizon) of this soil is indicative of some chemical weathering. It is probable that vermiculite formation from biotite mica has played an important role in grussification of parent rock.

Since vermiculite is considered a fast-forming, unstable intermediate from which smectite is known to form, the smectite present in these horizons probably represents a more stable alteration product of vermiculite (Kittrick, 1973; Borchardt, 1979). Kaolinite, in turn,

represents the most stable clay mineral found in the acidic, leaching environment of the eluvial horizons.

Some formation of smectite and vermiculite probably represents what little weathering has occurred in the C horizon. Grus present in this horizon reflects an early stage of development. Some breakdown of rock structure has occurred by a small amount of alteration to secondary clays in combination with physical processes such as freeze-thaw.

Clay mineralogy of the B horizons suggests some rather different weathering processes than those observed in the eluvial and C horizons. While smectite is present in the A21, A22, and C horizons, it is important to note that on a whole soil basis, it accounts for less than 1% of these horizons. However, in the B22t horizon, smectite accounts for approximately 23% of the soil solids.

In view of this and the mineral composition of Butte quartz monzonite, it is difficult to explain the amount of smectite in the argillic horizon as a pedogenic weathering product forming from micas. There is simply not enough biotite or clay-size mica (illite) present in the parent material to account for so much smectite.

Evidence for Pedogenic Weathering

Evidence for pedogenic weathering was seen in this study by SEM and thin section examination. This evidence provides some insight into the observed contrasts in clay mineralogy.

SEM imagery demonstrated the occurrence of pedogenic feldspar weathering in the soil profile. Dissolution pits on feldspar grains

were similar in appearance to those described by other researchers (Eswaran and Bin, 1978; Berner and Holdren, 1977; Wilson, 1975). These pits resulted from preferential weathering of less-resistant portions of the feldspar crystalline structure. This left behind the more resistant framework of the crystal lattice, resulting in a honeycomb appearance.

These dissolution pits are characteristic of the weathering of feldspars in soils (Berner and Holdren, 1977). Although weathering pits were observed in both A and B horizons, they did not occur extensively. Therefore, this type of feldspar weathering does not appear to be a likely source of the large quantity of smectite in the argillic horizon.

Examination of thin sections from the A21 and A22 horizons showed a general lack of significant mineral alteration and clay formation. Although original mineral grain size and arrangement was absent, quartz and orthoclase showed very little chemical alteration. Biotite, plagioclase, and hornblende were also relatively fresh, despite some small zones of weathering observed along fractures and mineral grain edges.

In short, weathering of minerals in eluvial horizons does not appear advanced enough to produce large amounts of smectite for leaching.

In fact, the role of eluviation and illuviation in the formation of this argillic horizon appears to be small. The mineralogy of the argillans taken from the B22t horizon showed illite to be the dominant clay mineral being moved.

Also, the illite content of the clay-size matrix component of the B22t soil fabric is lower than the illite content of the B22t horizon as a whole, where the matrix and clay films are combined. In other words, the high smectite content of the B22t horizon is not due to illuviation. Apparently, most of the smectite found in the B horizons has been formed in situ.

Evidence of Clay Illuviation

Evidence of an argillic horizon is clearly seen in this soil profile. Clay films observed in the field and by thin section microscopy do represent illuvial clay and not pressure faces. Mineralogy of these clay films is more similar to that of the eluvial horizons than to that of the B horizons. Therefore, these argillans likely represent clay which has been translocated from the A21 and A22 horizons into Bt horizons.

Particle size analysis showed that the Bt horizons have sufficient increases in clay-size material to meet criteria for an argillic horizon (Soil Survey Staff, 1975). Because a clay increase is apparent and illuviation has occurred, an argillic horizon as defined by Soil Taxonomy is present in this and similar soils.

Evidence of Hydrothermal Alteration

It is likely that hydrothermal alteration of the quartz monzonite and not pedogenic processes is primarily responsible for the high smectite contents found in the argillic horizons. The hypothesis that

hydrothermal argillization has occurred is based on findings in this study in addition to those of other researchers.

Material from the argillic horizon shows more intense alteration than overlying and underlying horizons when examined in thin section. Generally, intensity of weathering would be expected to decrease with depth in a soil profile. In this case, however, weathering in the surface horizons has been less intense than in the B horizons.

Plagioclase is noticeably absent from the B22t horizon and is intensely weathered in the B21t and B23t horizons. Alteration of plagioclase to secondary clay minerals by hydrothermal processes has been reported by several researchers on the Boulder and Idaho batholiths (Sales and Meyer, 1948; Becraft et al., 1963; Pinckney, 1965; Clayton et al., 1979).

In addition, the study area in this project is located in a large hydrothermally mineralized zone mapped by Pinckney (1965). This zone is a roughly circular area in the northern part of the Boulder batholith with a diameter of approximately 30 km.

The smectite-dominated clay mineralogy of the argillic horizon also differs markedly from the mineralogy observed in surface eluvial and C horizons. This mineralogy is also different from what is common in soils on granitic parent materials in similar environments (Veseth, 1981; Hood, 1963; Clayton et al., 1979). However, smectite has been reported by numerous researchers to dominate certain soils associated with areas of hydrothermal alteration (Grim, 1968).

The ghost rock inclusions have clay mineralogy similar to that of the argillic horizon. Thin section analysis showed the presence of

relict plagioclase grains in these inclusions. These relict grains are most likely smectite pseudomorphs of plagioclase.

Pseudomorphs provide strong evidence of weathering in place (Birkeland, 1974). Their presence in this profile indicates irregular zones of in situ weathering across the argillic horizon. Morphology and mineralogy of these zones are similar to zones characteristic of hydrothermal alteration.

Weathering is less intense in the ghost rocks than in the surrounding argillic horizon, suggesting these inclusions represent small zones of less intense hydrothermal argillization. Their location in the profile was probably dictated by the original micro-structure of cracks through which hydrothermal solutions circulated.

It is probable that smectite pseudomorphs of plagioclase were at one time present in the argillic horizon as well. Subsequent disturbance and mixing by roots, fauna, and the shrinking and swelling action of smectite itself has probably destroyed many of these relict grains.

The unusual diagonal orientation of the B3 horizon boundaries also suggests differential weathering zones resulting from hydrothermal processes. The B3 horizon probably does not have pedogenic origins. With mineralogy similar to that of the argillic horizon, the B3 probably represents the outermost fringe of hydrothermal activity.

Based on this evidence, the parent material in which this argillic horizon formed is presumed to have been partially argillized by hydrothermal processes. Hydrothermal alteration of quartz monzonite

has been shown to produce many of the mineralogical characteristics found in the B horizons of this soil.

Soil Genesis

In order to present a hypothesis explaining the genesis of this soil, it is necessary to consider the distinct mineralogical zones resulting from hydrothermal alteration of quartz monzonite (See Figure 1). This zone of hydrothermal alteration was located near the surface of the landscape and represented a horizontal extension of a larger, vertically-oriented vein of alteration extending downward far below the surface.

Following hydrothermal activity, erosion removed overlying material and exposed a landscape consisting of unaltered quartz monzonite covered with an irregular veneer of argillized material (Figure 14).

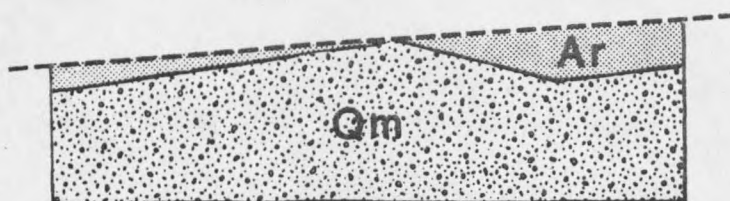


Figure 14. Landscape following removal of overlying altered zones. Ar = argillized zone; Qm = unaltered quartz monzonite

Deposition of slightly weathered quartz monzonite then followed. This material was derived from weathering of exposed, unaltered granitic rock present in the area. Deposition probably resulted from glacial or periglacial processes occurring during Wisconsin glaciation.

With establishment of coniferous vegetation and subsequent pedogenesis, a soil similar to the one studied was formed (Figure 15). The clear, smooth and wavy boundaries between the eluvial horizons and the hydrothermally altered B horizon reflect the depositional activity. By contrast, the irregular and broken boundaries between B horizons and the C horizons reflect former fringe zones of hydrothermal argillization.

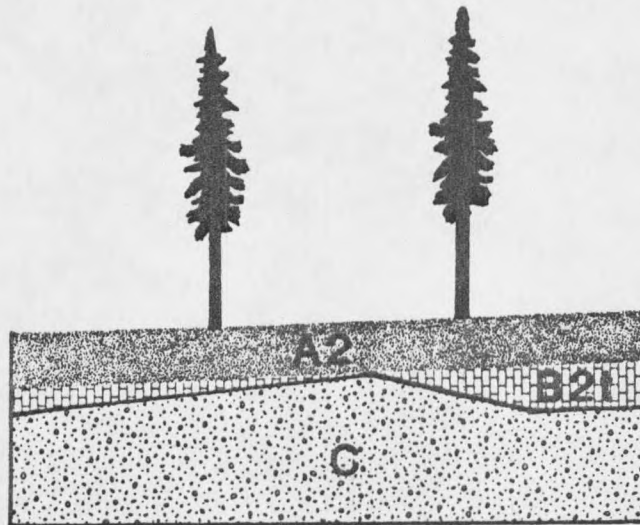


Figure 15. Soil horizon development following deposition, establishment of vegetation, and pedogenesis.

Although the processes resulting in formation of this soil are undoubtedly complex, this simple explanation does explain many of the results obtained in this study. This soil contains an argillic horizon exhibiting evidence of hydrothermal argillization upon which the effects of pedogenic processes of clay formation and translocation

have been superimposed. The B horizon differs markedly from the surface horizons in mineralogy and associated characteristics. Because of these differences, designation of a lithologic discontinuity between A and B horizons might be justified.

Hydrothermal Alteration and the Landscape

Although the relationships between soil properties and geomorphology of the study area was beyond the scope of this thesis project, brief mention of this subject seems appropriate. Similarities exist between this soil and those studied on the Idaho batholith where slope failures have been reported.

Argillization of quartz monzonite by hydrothermal processes appears to be a likely cause of poor drainage found in portions of the study area. It is also likely that poor drainage is at least partially responsible for processes such as solifluction and soil creep which have been active in the area.

Examination of several roadcuts in the study area revealed argillized zones rich in smectite. These zones occurred as far as 10 m below the soil surface. In addition, an exposed soil profile on a 50% ridge slope had a water table within 60 cm. of the soil surface. Material obtained from underneath this perched water table was rich in smectite.

Because of some of the physical properties associated with smectite minerals, soils developed in areas affected by hydrothermal activity could require special management. Logging and road-building

activity in this and similar areas could have unfavorable environmental and economic implications where these argillized zones are extensive.

Conclusions

A geochemical process, hydrothermal alteration of quartz monzonite, is primarily responsible for the chemical, physical, mineralogical, and morphological characteristics of the argillic horizon investigated here. Although pedogenic processes of clay formation and leaching have been sufficiently active to form an argillic horizon, their influence on these properties has been minimal.

LITERATURE CITED

LITERATURE CITED

- Becraft, G.E., D.M. Pinckney, and S. Rosenblum. 1963. Geology and mineral deposits of the Jefferson City quadrangle, Jefferson and Lewis and Clark Counties, Montana. U.S. Geol. Surv. Prof. Paper 428. pp 1-100.
- Berner, R.A and G.K. Holdren Jr. 1977. Mechanisms of feldspar weathering: some observational evidence. *Geology* 5: 369-372.
- Birkeland, P.W. 1974. Pedology, weathering, and geomorphological research. Oxford University Press, Inc., New York. 285 pp.
- Bisdorn, E.B.A. 1980. A review of the application of submicroscopic techniques in soil micromorphology. I. Transmission electron microscope (TEM) and scanning electron microscope (SEM). In E.B.A. Bisdorn (ed.) Submicroscopy of soils and weathered rocks. 1st Workshop of the International Working Group on Submicroscopy of Undisturbed Soil Materials (IWGSUSM). Wageningen, The Netherlands. pp 67-117.
- Borchardt, G.A. 1979. Montmorillonite and other smectite minerals. In J.B. Dixon and S.B. Weed (eds.) Minerals in soil environments. Soil Sci. Soc. Am., Madison, WI. pp 293-330.
- Bremner, J.M. 1965. Total nitrogen. In C.A. Black et al. (eds.) Methods of soil analysis, Part 2. *Agronomy* 9:1171-1175. Am. Soc. Agron., Madison, WI.
- Chapman, H.D. 1965a. Total exchangeable bases. In C.A. Black et al. (eds.) Methods of soil analysis, Part 2. *Agronomy* 9: 902-904. Am. Soc. Agron., Madison, WI.
- Chapman, H.D. 1965b. Cation exchange capacity. In C.A. Black et al. (eds.) Methods of soil analysis, Part 2. *Agronomy* 9: 891-901. Am. Soc. Agron., Madison, WI.
- Clayton, J.L. 1974. Clay mineralogy of soils in the Idaho batholith. *Geol. Soc. Amer. Bull.* 85:229-232.
- Clayton, J.L., W.F. Megahan, and D. Hampton. 1979. Soil and bedrock properties: weathering and alteration products and processes in the Idaho batholith. USDA Forest Service Res. Paper INT-27. 35 pp.

- Day, P.R. 1965. Hydrometer method of particle size analysis. In C.A. Black et al. (eds.) Methods of soil analysis, Part 1. Agronomy 9:562-567. Am. Soc. Agron., Madison, WI.
- Douglas, L.A. 1979. Vermiculites. In J.B. Dixon and S.B. Weed (eds.) Minerals in soil environments. Soil Sci. Soc. Am., Madison, WI. pp 259-292.
- Eswaran, H. and Wong Chaw Bin. 1978. A study of a deep weathering profile on granite in Peninsular Malaysia, III. Alteration of feldspars. Soil Sci. Soc. Am. J. 42(1):154-158.
- FitzPatrick, E.A. 1980. The micromorphology of soils. A manual for the preparation and description of thin sections of soils. Department of Soil Science, University of Aberdeen. 229 pp.
- Grim, R.F. 1968. Clay mineralogy. McGraw-Hill Book Co., New York. 596 pp.
- Guilbert, J.M. and R.L. Sloane. 1968. Electron-optical study of hydrothermal fringe alteration of plagioclase in quartz monzonite, Butte District, Montana. Clays Clay Miner. 16:215-221.
- Hood, W.C. 1963. Weathering of the Butte quartz monzonite near Butte, Montana: PhD dissertation. Montana State University. 88 pp.
- Isherwood, D. and A. Street. 1976. Biotite-induced grussification of the Boulder Creek granodiorite, Boulder County, Colorado. Geol. Soc. Am. Bull. 87:366-370.
- Jackson, M.L. 1956. Soil chemical analysis--advanced course. University of Wisconsin, Madison. 991 pp.
- Jackson, M.L. 1959. Frequency distribution of clay minerals in major Great Soil Groups as related to the factors of soil formation. Proceedings of the 6th National Clay Conference. Pergamon Press, New York. pp 133-143.
- Jenny, H. 1935. The clay content of the soil as related to climatic factors, particularly temperature. Soil Sci. 40:111-128.
- Kaczmarek, M.B. 1974. Geothermometry of selected Montana hot spring waters. MS thesis. Montana State University, Bozeman. 141 pp.
- Kittrick, J.A. 1973. Mica-derived vermiculites as unstable intermediates. Clays Clay Miner. 21:479-488.
- Klages, M.G. and R.W. Hopper. 1982. Clay minerals in northern plains coal overburden as measured by x-ray diffraction. Soil Sci. Soc. Am. J. 46:415-419.

- Marchand, D.E. 1974. Chemical weathering, soil development, and geochemical fractionation in a part of the White Mountains, Mono and Inyo Counties, California. U.S. Geol. Surv. Prof. Pap. 352-J. pp 379-434.
- McKeague, J.A. and R.J. St. Arnaud. 1969. Pedotranslocation: eluviation-illuviation in soils during the Quaternary. Soil Sci. 107:428-434.
- Millot, G. 1979. Clay. Scientific American 240(4):109-119.
- Moorhouse, W.W. 1959. The study of rocks in thin section. Harper and Row Publishers, New York. 574 pp.
- Munn, L.C. and G.A. Nielsen. 1979. Soil temperature predictions in mountains and foothills of Montana. Montana Agr. Exp. Sta. Bull. 705.
- Nettleton, W.D., K.W. Flach, and G. Borst. 1968. A toposequence of soils in tonalite grus in the southern California Peninsular Range. USDA Soil Survey Inv. Report No. 21.
- Nettleton, W.D., K.W. Flach, and B.R. Brasher. 1969. Argillic horizons without clay skins. Soil Sci. Soc. Am. Proc. 33:121-125.
- Perry, E.S. 1962. Montana in the geologic past. Mont. Bur. Mines Geol. Bull. 26:34-38.
- Pfister, R.D., B.L. Kovalchik, S.F. Arno, and R.C. Presby. 1977. Forest habitat types of Montana. USDA Forest Service Gen. Tech. Rep. INT-34. 174 pp.
- Pinckney, D.M. 1965. Veins in the northern part of the Boulder batholith, Montana. U.S. Geol. Surv. Open-file Rep. 153 pp.
- Ruppel, E.T. 1962. A Pleistocene ice sheet in the northern Boulder Mountains, Jefferson, Powell, and Lewis and Clark Counties, Montana. U.S. Geol. Surv. Bull. 1141-G. 22 pp.
- Ruppel, E.T. 1963. Geology of the Basin Quadrangle. Jefferson, Lewis and Clark, and Powell Counties, Montana. U.S. Geol. Surv. Bull. 1151. 121 pp.
- Sales, R.H. and C. Meyer. 1948. Wall rock alteration at Butte, Montana. Am. Inst. Mining Met. Engrs. Trans. 178:1-35.
- Sims, J.R. and V.A. Haby. 1971. Simplified colorimetric determination of soil organic matter. Soil Sci. 112:137-141.

- Smedes, H.W. 1966. Geology and igneous petrology of the northern Elkhorn Mountains, Jefferson and Broadwater Counties, Montana. U.S. Geol. Surv. Prof. Pap. 510. 116 pp.
- Soil Survey Staff. 1951. Soil survey manual. USDA Handbook No. 18. U.S. Government Printing Office, Washington, D.C.
- Soil Survey Staff. 1975. Soil taxonomy. USDA Handbook No. 436. U.S. Government Printing Office, Washington, D.C.
- Thiesen, A.A. and M.E. Harward. 1962. A paste method for preparation of slides for clay mineral identification by x-ray diffraction. Soil Sci. Soc. Am. Proc. 26:90-91.
- Tilling, R.I., M.R. Klepper, and J.D. Obradovich. 1968. K-Ar ages and time of emplacement of the Boulder batholith, Montana. Amer. J. Sci. 226:671-689.
- U.S. Salinity Laboratory Staff. 1969. Diagnosis and improvement of saline and alkali soils. USDA Handbook No. 60. U.S. Government Printing Office, Washington, D.C.
- Veseth, R.J. and C. Montagne. 1980. Geologic parent materials of Montana soils. Mont. Agr. Exp. Sta. Bull. 721. 117 pp.
- Veseth, R.J. 1981. Contrasting soil development on the sedimentary Kootenai formation and granitic Boulder batholith in southwestern Montana. MS thesis. Montana State University, Bozeman. 183 pp.
- Warhaftig, C. 1965. Stepped topography of the Sierra Nevada, California. Geol. Soc. Am. Bull. 76:1165-1190.
- Whittig, L.D. 1965. X-ray diffraction techniques for mineral identification and mineralogical composition. In C.A. Black et al. (eds.) Methods of soil analysis, Part 1. Agronomy 9: 671-698. Am. Soc. Agron., Madison, WI.
- Wilson, M.J. 1975. Chemical weathering of some primary rock-forming minerals. Soil Sci. 119:349-355.

APPENDICES

APPENDIX I
SOIL PROFILE AND SITE DESCRIPTION

CLASSIFICATION: fine-loamy over sandy, mixed Mollic Cryoboralf
 LOCATION: NW 1/4 SW 1/4 Sec 4 T5N R5W
 PHYSIOGRAPHIC POSITION: convex ridge slope
 ELEVATION: 1950 m (6400 ft)
 SLOPE AND ASPECT: 18 %, south
 VEGETATION: Douglas fir, lodgepole pine, pinegrass, kinnikinnick
 SAMPLED BY: P. McDaniel and C. Mogen, November, 1980

Colors are for crushed peds

- 01, 02 2-0 cm. Needles, twigs, and decayed organic material.
- A1 0-2 cm. Dark brown (10 YR 4/3) sandy loam, very dark brown (10 YR 2/2) moist; moderate very fine granular structure; soft, very friable, nonsticky and nonplastic; common very fine and very fine roots; clear smooth boundary.
- A21 2-15 cm. Light brownish gray (10 YR 6/2) sandy loam, dark yellowish brown (10 YR 3/4) moist; weak fine subangular blocky structure; loose, very friable, nonsticky and nonplastic; common very fine, fine, medium, and coarse roots; clear, smooth boundary.
- A22 5-28 cm. Light gray (10 YR 7/2) sandy loam, dark yellowish brown (10 YR 3/4) moist; weak fine subangular blocky structure; loose, very friable, nonsticky and nonplastic; common very fine, fine, medium, and coarse roots; clear, wavy boundary.
- B21t 28-37 cm. Yellowish brown (10 YR 5/4) sandy loam, dark yellowish brown (10 YR 3/4) moist; weak medium subangular blocky structure; slightly hard, friable, slightly sticky and slightly plastic; common fine, medium, and coarse roots; clear broken boundary.
- B22t 28-45 cm. Yellowish brown (10 YR 5/6) sandy clay loam, dark yellowish brown (10 YR 3/6) moist; strong medium prismatic structure; very hard, friable, sticky and plastic; common fine, medium, and coarse roots; common moderately thick clay films on ped faces; clear broken boundary.
- B23t 45-60 cm. Yellowish brown (10 YR 5/6) sandy clay loam, dark yellowish brown (10 YR 4/6) moist; moderate fine prismatic structure; very hard, friable, sticky and plastic; few fine and common medium and coarse roots; few moderately thick clay films on ped faces; clear broken boundary.
- B3 60-90 cm. Brownish yellow (10 YR 6/8) sandy loam, dark yellowish brown (10 YR 4/6) moist; weak medium subangular structure; slightly hard, very friable, slightly sticky and slightly plastic; few fine and common medium and coarse roots; clear broken boundary.

C 90+ cm. Yellowish brown (10 YR 5/4) loamy sand; structureless--single grain; loose, nonsticky and nonplastic; boundary not reached.

REMARKS

Organic staining can be seen on ped faces in B22t and B23t horizons. Two ghost rocks are seen in B22t and B23t horizons. The first of these inclusions, ghost rock 1, is located in the center of the profile at a depth of 45 cm. It is approximately 15 cm in diameter, slightly sticky and slightly plastic, and is pale brown (10 YR 6/3 dry). Ghost rock 2 is located at a depth of approximately 60 cm. It is slightly sticky and slightly plastic, and is light brownish yellow (10 YR 6/4 dry).

APPENDIX II
PHYSICAL LABORATORY DATA

HORIZON	DEPTH (cm)	% >2mm (by wt)	% OF FINE-EARTH FRACTION							TOTAL			% WATER		
			v coarse 1-2mm	coarse .5-1mm	SAND medium .25-.5mm	fine .1-.25mm	v fine .05-.1mm	SAND .05-2mm	SILT .002-.05mm	CLAY <.002mm	SAT.	123 bar	15 bar		
A1	0-2	17.7	18.6	27.1	5.0	14.3	7.1	71.4	22.2	6.4	42.8	15.9	6.3		
A21	2-15	23.6	19.4	22.8	4.2	15.2	7.6	69.2	24.4	6.4	21.1	10.1	3.5		
A22	15-28	16.4	14.4	22.7	2.8	19.3	9.6	68.8	23.1	8.1	22.1	9.8	4.1		
B21t	28-37	21.7	16.8	22.4	3.7	13.1	6.2	62.2	18.0	19.8	34.1	14.9	9.4		
B22t	28-45	15.7	9.0	18.0	1.7	18.0	9.6	56.2	16.2	27.6	45.5	20.9	10.8		
B23t	45-60	16.8	13.9	23.6	1.4	19.4	11.8	69.3	14.4	16.3	39.7	15.9	9.5		
B3	60-90	14.8	15.1	22.6	3.8	21.8	12.0	76.4	16.1	7.5	26.1	10.3	5.8		
C	90+	39.6	31.0	35.6	3.6	16.4	5.5	91.2	7.2	1.6	15.1	3.5	1.4		
Ghost Rock 1	45	16.4	-	-	-	-	-	74.9	17.2	7.9	15.4	9.1	4.0		
Ghost Rock 2	60	10.6	-	-	-	-	-	68.5	22.9	8.6	28.9	10.5	6.2		

APPENDIX III
CHEMICAL LABORATORY DATA

HORIZON	pH (1)	EC mmhos/cm (2)	% NITROGEN	% ORGANIC MATTER	EXTRACTABLE BASES (3) (me/100s)				SOLUBLE BASES (2) (me/l)				CEC (4) me/100s	SAR (5)	% BASE SATURATION (6)
					Ca	Mg	Na	K	Ca	Mg	Na	K			
A1	5.4	0.9	.102	6.8	5.1	0.9	0.1	0.5	2.8	1.0	0.3	0.9	14.6	0.2	44
A21	4.8	0.2	.032	0.4	2.2	0.8	0.1	0.2	1.0	0.4	0.4	0.3	8.1	0.5	40
A22	5.0	0.2	.031	0.5	3.8	1.3	0.1	0.3	1.0	0.4	0.4	0.3	9.4	0.5	58
B21t	5.3	0.3	.026	0.5	12.8	4.3	0.1	0.6	1.7	0.7	0.3	0.6	21.2	0.3	83
B22t	5.3	0.2	.024	0.7	20.0	7.6	0.1	0.7	1.0	0.5	0.3	0.4	31.9	0.3	89
B23t	5.7	0.3	.026	<0.1	14.6	4.9	0.1	0.4	3.0	1.3	0.3	0.3	24.5	0.2	81
B3	6.3	0.2	.007	<0.1	8.8	2.8	0.1	0.2	0.6	0.3	0.3	0.1	14.8	0.4	80
C	6.1	0.1	.004	<0.1	4.6	1.4	0.1	0.2	0.5	0.2	0.3	0.1	9.3	0.5	67
Ghost Rock 1	6.2	0.1	.007	<0.1	5.1	1.6	0.1	0.2	0.5	0.2	0.3	0.2	9.7	0.5	76
Ghost Rock 2	6.2	0.1	.007	<0.1	9.9	3.2	0.1	0.2	0.7	0.3	0.3	0.1	15.7	0.4	85

58

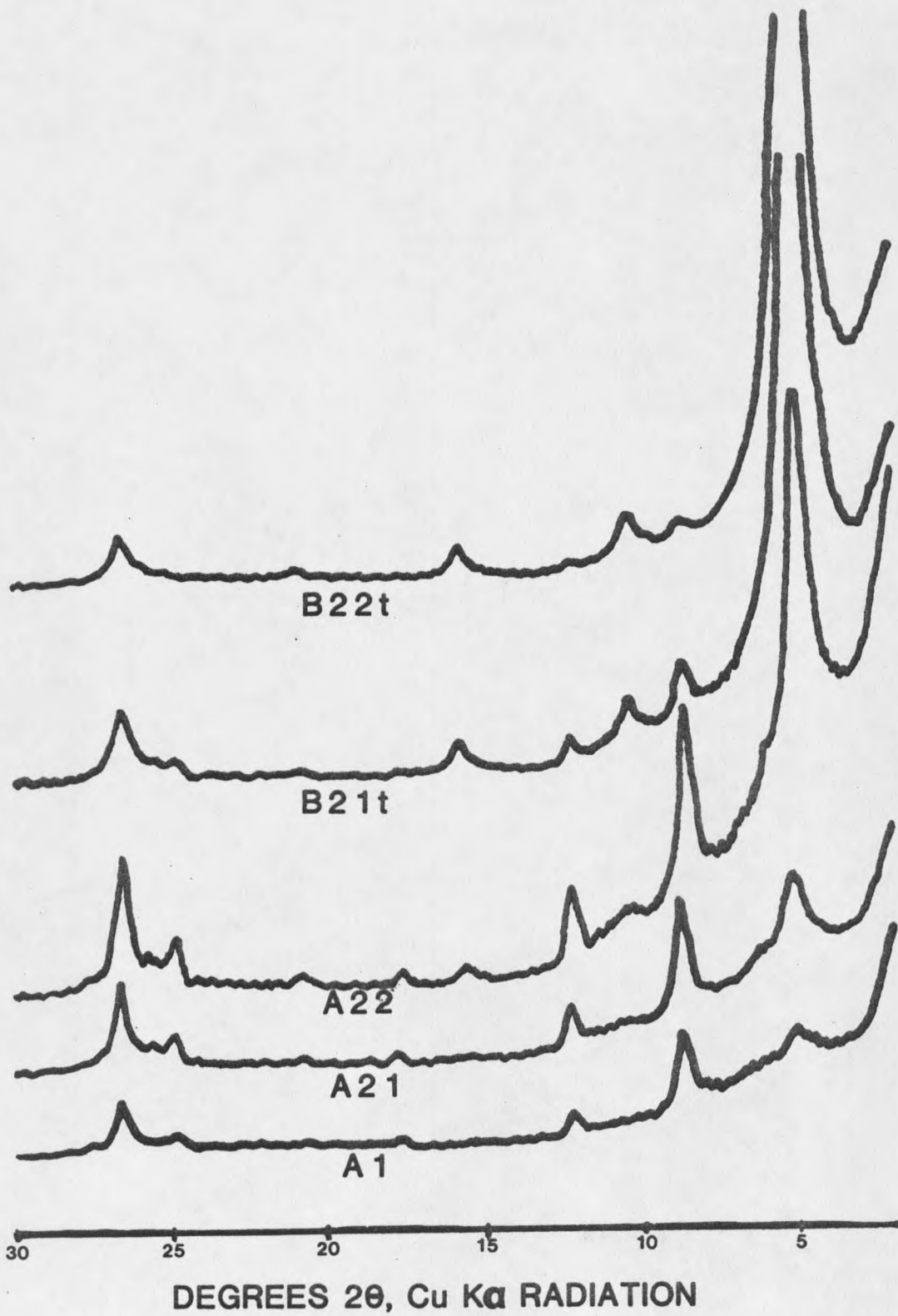
- (1) saturated paste
(2) saturated paste extract
(3) 1 N NH4OAc extract
(4) NaOAc saturation

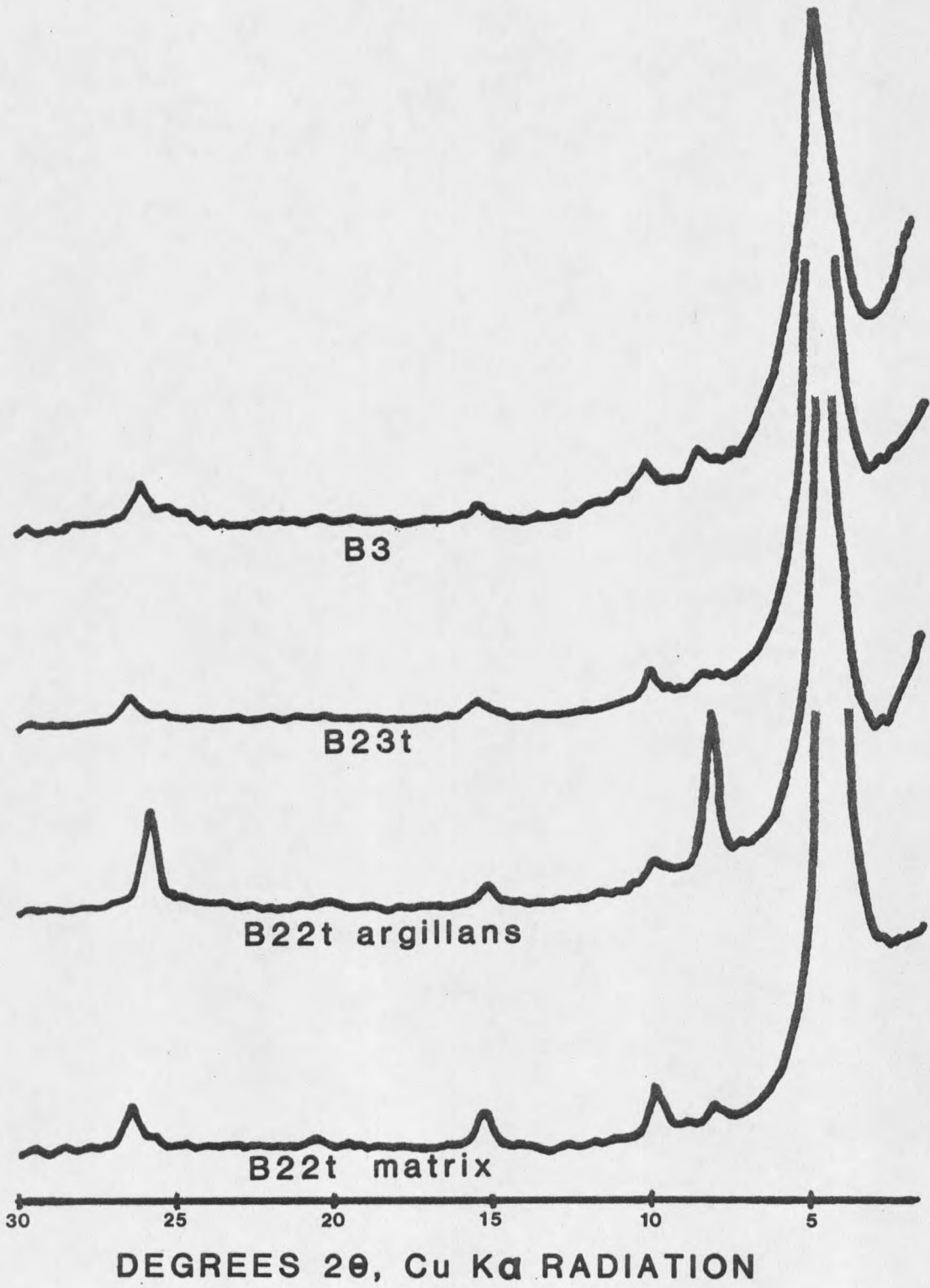
$$(5) \text{ Sodium Adsorption Ratio} = \frac{\text{Na}}{\sqrt{\frac{\text{Ca} + \text{Mg}}{2}}}$$

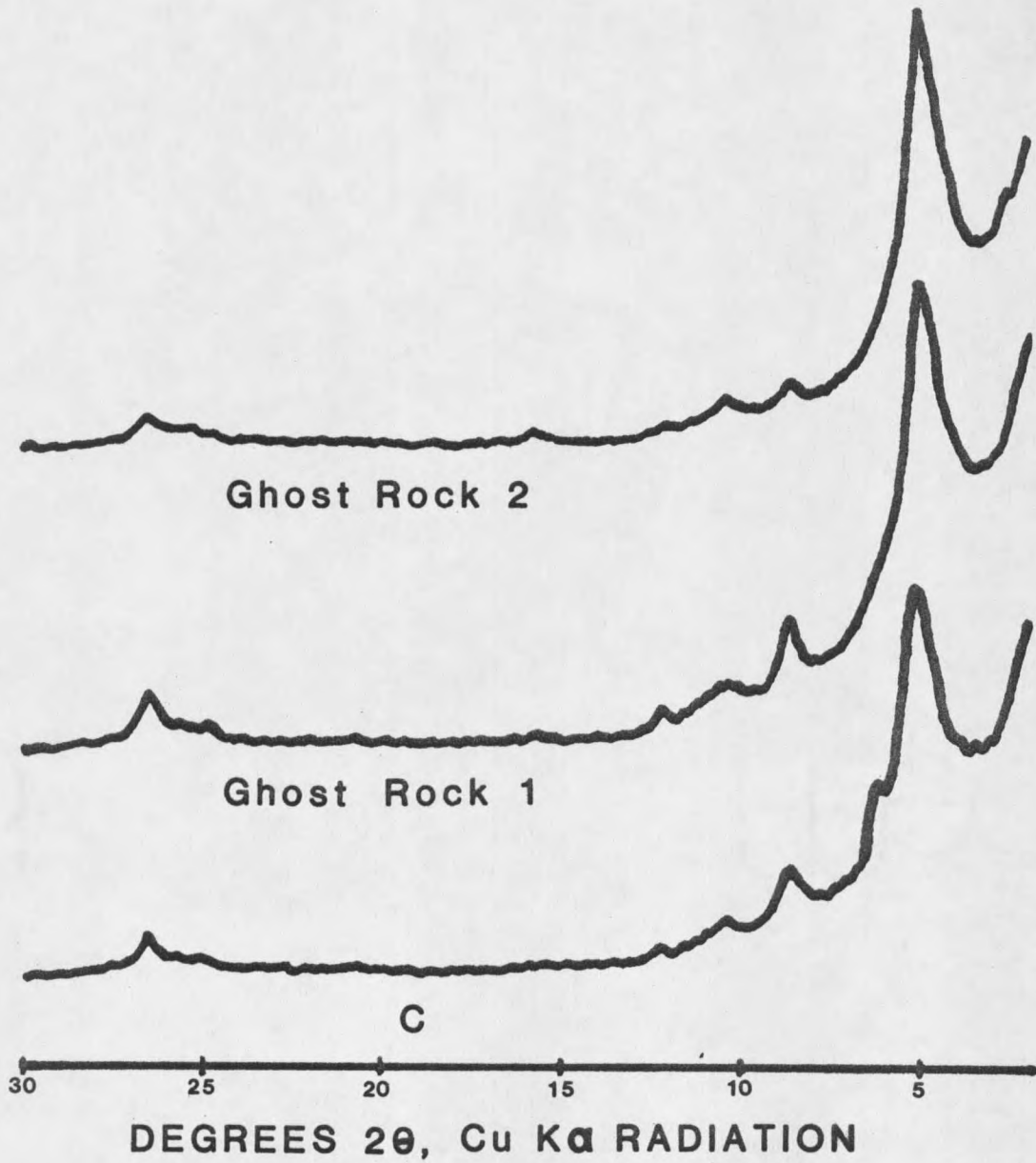
$$(6) \% \text{ Base Saturation} = \frac{\text{Sum of exchangeable bases}}{\text{CEC}} \times 100$$

APPENDIX IV

X-RAY DIFFRACTION PATTERNS FOR MG-SATURATED, ETHYLENE
GLYCOLSOLVATED CLAY FRACTIONS







APPENDIX V
ESTIMATED CLAY MINERAL PERCENTAGES

Percent of Clay-size Fraction

<u>Sample</u>	<u>Smectite</u>	<u>Illite</u>	<u>Vermiculite</u>	<u>Kaolinite</u>	<u>Quartz</u>
A21	9	79	3	9	-
A22	18	69	3	10	-
B21t	60	26	-	3	11
B22t	83	14	-	1	3
B23t	81	14	-	-	5
B3	71	24	-	2	3
C	32	52	7	-	9
Clay Films	42	58	-	-	-
B22t Matrix	87	7	-	-	6
Ghost Rock 1	57	38	-	3	2
Ghost Rock 2	67	16	-	12	5

